ELSEVIER

About process times in some deepwater formation events in the Mediterranean Sea

V. Bouché*

Physics Department, "La Sapienza" University, Rome, Italy

Abstract

Experimental data gathered on some Mediterranean deepwater formation sites have been analysed in order to check the Chapman (Ch), Visbeck and Maxworthy scale laws, their final mixing water depth and process times estimates. All the analysed sites have a high probability to be "internally constrained" so that the baroclinic Rossby radius is the dominant horizontal length scale and the final chimney depth is independent of the rate of rotation as indicated by Visbeck and Maxworthy criteria; the Eady instability times are generally very fast ($\sim 3/f$) but the least final mixing process times are too long compared with the meteorological forcing ones. It is attempted here to identify some new criteria to give some insight on the processes time scale, which is still an open problem. Conclusions about the Rhodes gyre appear questionable, because the experimental data appear inconsistent with any theoretical criterion.
© 2002 Elsevier Science B.V. All rights reserved.

Keywords: Deep convection; Dense water; Mediterranean Sea; Baroclinic instabilities; Rossby radius; Surface buoyancy flux; Field data errors

1. Introduction

In recent times, the dense water formation (DWF) process (Killworth, 1983) in the sea has been one of the more extensively studied questions. It is generally accepted that a localized convective process due to an outward surface buoyancy flux is one of the principal mechanisms setting it up (Maxworthy, 1997) when very strong, dry cool winds are blowing in the open sea surface during the late winter. The Mediterranean Sea is a natural laboratory basin where many deepwater formation sites have been localized (Fig. 1).

Many experimental data from field observations gathered during sea surveys and satellite observations (Gremes-Cordero, 1999) have documented some periods and sites where these phenomena occur (MEDOC Group, 1970; Schott and Leaman, 1991; Schott et al., 1993, 1994, 1996; Georgopoulos et al., 1989; Bunker, 1972; Anati, 1984; Gertman et al., 1994; Lascaratos, 1993; Ovchinnikov et al., 1985; Ozturgut, 1976; Roether et al., 1996; Manca and Bregant, 1998; Spernocchia et al., 1995; Sur et al., 1992). It is then useful to have some DWF criteria from which to forecast the sites, the periods and the depths of the new dense water, from the knowledge of a few macroscopic experimental data. Tank and numerical experiments, so as theoretical analyses (Maxworthy and Narimousa, 1994; Narimousa, 1996; Visbeck et

* Fax: +39-06-4454749.
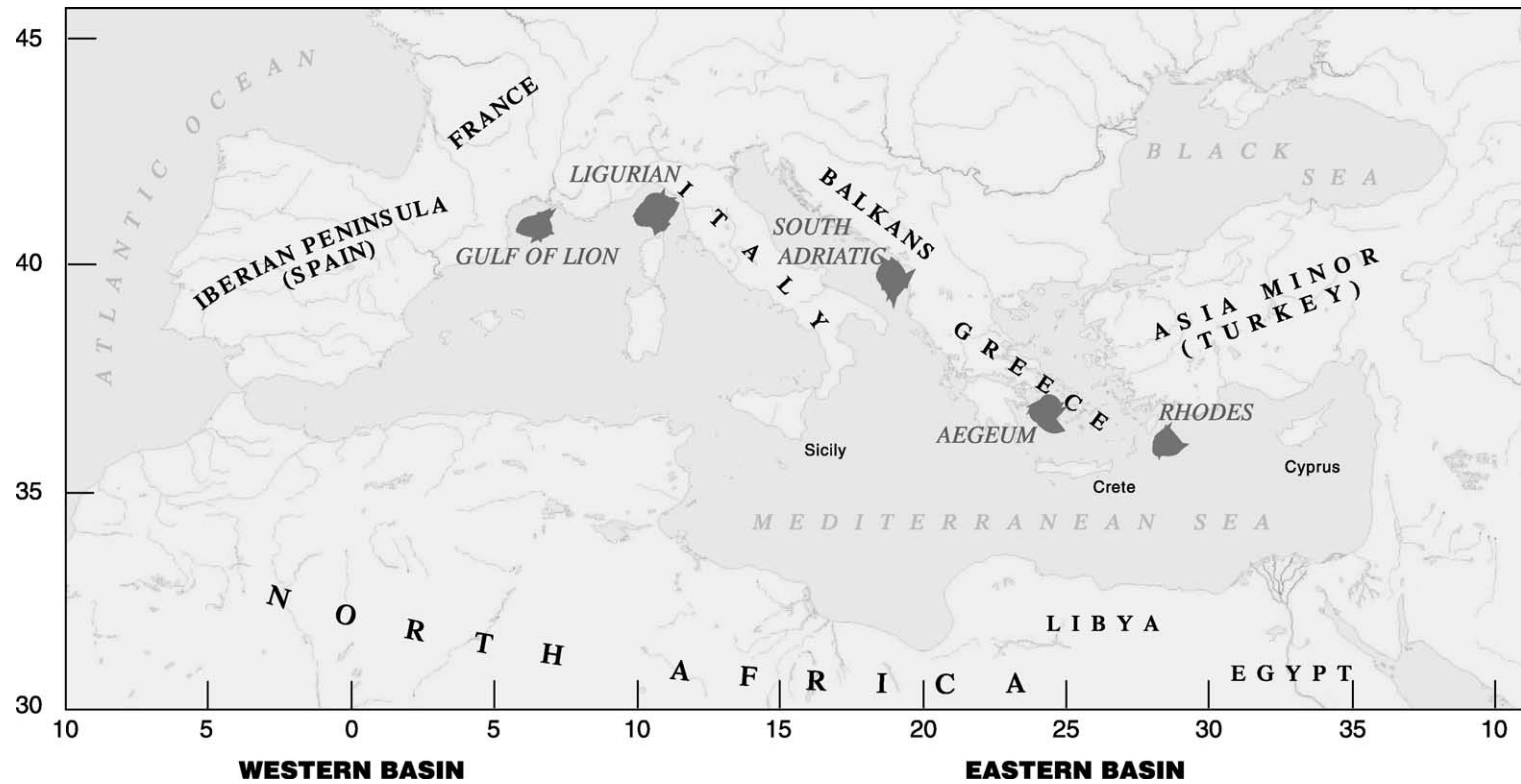*E-mail address:* vanda.bouche@roma1.infn.it (V. Bouché).

Fig. 1. A map with the locations of deepwater formation sites in the Mediterranean Sea analysed herein.

al., 1996; Tzipermann, 1996; Chapman, 1998; Marshall et al., 1994; Marshall and Schott, 1998) have led to the formulation of some of these scale laws. The experimental observations can be summed up in four phases: a preconditioning (or doming formation) phase, a violent mixing (or plume formation) phase, a plume mixing (or rotating chimney formation) phase, a chimney baroclinic instability (or cone formation) phase until, as the external forcing dies down, the chimney finally breaks down (restratification phase) on a slow time scale compared with the formation times, variable depending on the site and on the event $[O (10–10^2)$ days], but such that increased deep density variance on a larger scale continues to exist well into the next summer, allowing identification of previous winter convection activity (Schott et al., 1994). Each of these stages is ruled by its own scale laws, but their dynamics are far from being fully understood (Send and Marshall, 1995; Jones and Marshall, 1993). Recently, considerable attention was focused on the chimney scale, namely the effect of many "1-km" large plumes that are thought to be efficient water mixing agents, and on the role of geostrophic eddies that develop in the baroclinic zone on the periphery of the chimney, controlling the exchange of fluid between the chimney and its surroundings. This last phenomenon (corresponding to the fourth of the above-mentioned phases) has been thoroughly studied by Visbeck et al. (1996) (VMJ), Chapman (1998) (Ch), Coates et al. (1995), Maxworthy and Narimousa (1994) and Narimousa and Maxworthy (1994) (MN) through tank experiments and numerical simulations. The common theoretical assumption is that as the chimney grows in density, it deepens, forming a homogeneous density front between the chimney and the surrounding water; if the chimney is large enough that the Burger number is $Bu \ll 1$ (i.e. the radius of the chimney is greater than the Rossby deformation radius), the front is subject to baroclinic instability and breaks up into eddies whose velocities scale like the rim current velocity in geostrophic equilibrium, according to the thermal wind law, till a quasi steady condition is reached, when the surface buoyancy loss is fully balanced by the lateral eddy flux of buoyancy through the sides of the convective chimney. This state can be reached if the time of mixing and deepening process is shorter than the forcing time. This assumption allows very simple

laws to be formulated for the times and the depths of the process if the stratification $N^2 = (− (g/\rho_0))((d\rho_0(z)/dz))$, assumed as constant, the average surface buoyancy flux B_0, assumed as homogeneous and constant, and the horizontal dimensions of the cooling event, assumed as circular, are known (VMJ; MN). However, it is possible to envisage other laws if certain changes are made in the model.

In particular, Chapman (Ch) studied the consequences of the nonhomogeneity of the surface buoyancy flux by allowing the latter to have a linear decay towards zero in a narrow zone on the boundary; he inferred that the average homogeneous buoyancy flux B_0 is the only parameter affecting the scale law (which does not depend on the Coriolis parameter f) if the deepening process and the transient are so slow that the equilibrium condition is reached when the dimension of the Rossby deformation radius has grown to a value higher than the external horizontal variability region of the buoyancy flux (internally constrained convection). However, if the deepening process is so fast and the transient so short that the equilibrium condition is reached when the deformation Rossby radius is smaller than the external decay region, then the scale law is also constrained by the size of the external boundary region W and by the Coriolis parameter (externally constrained convection). The transition between the two kinds of convection occurs, in the case of high stratification and deep convection, at a time (Chapman, 1998, Eq. (24)) where:

$$t^* \approx \frac{f^2 W^2}{B_0} \frac{8}{9} \tag{1}$$

The convection is externally constrained if the process time is $t_f \ll t^*$, and internally constrained if $t_f \gg t^*$. Numerical calculations show (Ch) that the transition is smooth, so there is some range of intermediate cases for which neither set of scales applies precisely. This transition time (Eq. (1)), compared to the time of the process (Eq. (8c)), corresponds to a value of W (Ch), such that $W/R_0 \approx n_t$, where:

$$n_t = \left(\frac{9}{8}\right)^{2/3} \left(\frac{1}{2\alpha}\right)^{1/3} \left(\frac{B_0}{f^3 R_0^2}\right)^{1/3} \tag{2}$$

Here, W is the dimension of the external boundary region, R_0 is the homogeneous buoyancy flux radius

in a circular geometry, f is the Coriolis parameter, B_0 the homogeneous surface buoyancy flux, $(B_0/f^3)^{1/2} = l_{rot}$ is the vertical length scale over which rotation becomes important in the sinking process (Jones and Marshall, 1993), and $\alpha = 0.013$ is a correlation parameter between the eddy velocities and the density anomaly, measuring the efficiency of the flow transport through the edge line. The convection is externally constrained if $W/R_0 \gg n_t$, but internally constrained if $W/R_0 \ll n_t$.

Buongiorno-Nardelli and Salusti (1999) (BNS) analysed known experimental data for deepwater formation in some regions of the Mediterranean Sea to be compared to the depths estimated by the Visbeck (VMJ) and Maxworthy (MN) criteria. They infer that the measured and computed values coincide within the error proposed in the VMJ and MN models even if their data may not represent the best data set imaginable. In any case, they can infer where deep or intermediate or near surface water formation sites are placed. But a more general analysis, including the Ch criterion and the times of the process, has not yet been done. In this paper, our intention is to carry out this deeper and more general analysis in order to check the consistency of these criteria and to reach more definite conclusions. Particular stress is given to the analysis of the expected process times (transition time, final mixing time, Eady time, restratification time) in order to compare them with each other and to the meteorological external forcing times and to check the consistency of the models according to the theoretical analysis. At last, a correction of the theoretical formulas inside the same model will be tried; this, taking into account the preconditioning, reduces the minimum final mixing times, and makes them consistent with the meteorological times.

2. A summary of the criteria

As mentioned above, all criteria are based on the fundamental assumption that a quasi steady state is reached when the surface buoyancy flux is balanced by the lateral time-averaged buoyancy flux due to a baroclinic instability on the chimney's boundary (VMJ; Ch; MN; Coates et al., 1995). As the chimney deepens, the isopycnals become steeper and steeper; the potential energy stored in the sloping region

(baroclinic instability zone) is converted into kinetic energy along the chimney boundary so that eddy motions begin; as the baroclinic region grows (as does the isopycnal sloping), the eddies increase and become more intense, exchanging the chimney water with the surrounding water; a quasi steady state is reached when the incoming and outgoing water flux is such that an incoming turbulent eddy buoyancy flux halts density growth in the chimney and the latter's deepening. The velocity of the vortices is ruled by the thermal wind law and scales like the rim current at the boundary of the chimney in geostrophic equilibrium. No discontinuity in density at the base of the chimney is assumed.

VMJ analyse a chimney forced by homogenous surface buoyancy flux B_0 in a circular region with radius R_0 in a stratified sea with $N = \text{const}$; their theoretical scale law for the final chimney depth is:

$$h_f = \beta \frac{(B_0 R_0)^{1/3}}{N}, \quad \text{where } \beta = 3.9 \pm 0.9 \qquad (3)$$

This value of β was determined by laboratory and numerical experiments. The corresponding final quasi steady density anomaly is (VMJ):

$$\Delta \rho_f = \beta \frac{\rho_0 N}{g} (B_0 R_0)^{1/3} = \frac{\rho_0}{g} N^2 h_f \qquad (4)$$

The final equilibrium time (i.e. the time spent to reach this state) is given by (VMJ):

$$t_f \geq \frac{1}{2} \beta^2 \left(\frac{R_0^2}{B_0} \right)^{1/3} \qquad (5)$$

Numerical calculations (VMJ) set a final time $t_f = (12 \pm 3)(R_0^2/B_0)^{1/3}$. A correction to these scale laws has been given by MN: they studied the same physical model through tank experiments, and determined a slightly different value for the efficiency parameter:

$$\beta = 3.5 \pm 0.2 \qquad (6)$$

Ch studied a not very different but more realistic physical model by considering a circular forcing region with uniform buoyancy flux B_0 within a radial distance R_0, surrounded by a forcing decay region W wide, across which the buoyancy flux decreases

linearly from B_0 to zero, so that the surface buoyancy flux is:

$$
\begin{cases}
B_0 & r < R_0 \\
B_0(R_0 + W - r)/W & R_0 < r < R_0 + W = R \quad (7) \\
0 & r > R_0 + W = R
\end{cases}
$$

where r is the radial distance from the center of the forcing region. In this case, he obtains:

$$
h_f = \left(\frac{2}{\alpha}\right)^{1/4} \frac{1}{N} (fB_0R_0W)^{1/4} \qquad (8a)
$$

$$
\Delta\rho_f = \left(\frac{2}{\alpha}\right)^{1/4} \frac{\rho_0 N}{g} (fB_0R_0W)^{1/4} \qquad (8b)
$$

$$
t_f \geq \left(\frac{1}{2\alpha}\right)^{1/2} \left(\frac{fR_0W}{B_0}\right)^{1/2} \qquad (8c)
$$

where $\alpha = 0.013$ has been derived numerically (Ch).

Ch draws the conclusion that the scale laws (Eqs. (8a)–(8c)) are good if the internal Rossby radius during the quasi steady state is:

$$
R_d = Nh_f/f \ll W < R_0 \qquad (9)
$$

(externally constrained processes), but the VMJ or MN scale laws, i.e. Eqs. (3)–(5), are good if $R_0 \gg R_d > W$ (internally constrained process). In fact, the thermal wind law governing these processes links the horizontal density gradient on the baroclinic zone with the vertical velocity gradient. The scale laws are thus dependent on the horizontal density gradient scale; the Rossby radius depends on the density difference across the frontal region so that it grows in time and the forcing decay region width W thus fixes the scale of the horizontal density gradient till $R_d > W$. The transition between the two different regimes is given by Eqs. (1) and (2), depending on the buoyancy flux and on the radius of the chimney, but not on the stratification or on the final depth. It is noticeable at glance that in a well-stratified sea like the Mediterranean Sea, where $f \simeq 1.3 \times 10^{-4}$ s^{-1}, the condition (9) limits the externally constrained process likelihood to intermediate or levantine formation events unless W is large enough.

3. Comparing the criteria with experimental data

Both criteria, as explained in Eqs. (3) and (8a), give the dense water depth as a function of the surface buoyancy flux (assumed homogeneous and constant), the stratification before the storm (assumed constant), and the radius of the chimney (assumed circular). Moreover, the Coriolis parameter and the surface buoyancy flux decay region can affect it in the Chapman model. These have to be compared with the real situation of a preconditioned sea over which a violent storm cools and dries off a localized region of trapped water. A comparison between the theoretical laws and the experimental data set is by no means trivial; an agreement about the appropriate quantities to measure in order to calculate Eqs. (3) and (8a) is first required. The choice of the Coriolis parameter ($f \approx 10^{-4}$ s^{-1}) is immediate because of the extreme localization of the event; the final penetration depth of dense water h_f is fixed for every event and can be obtained by field
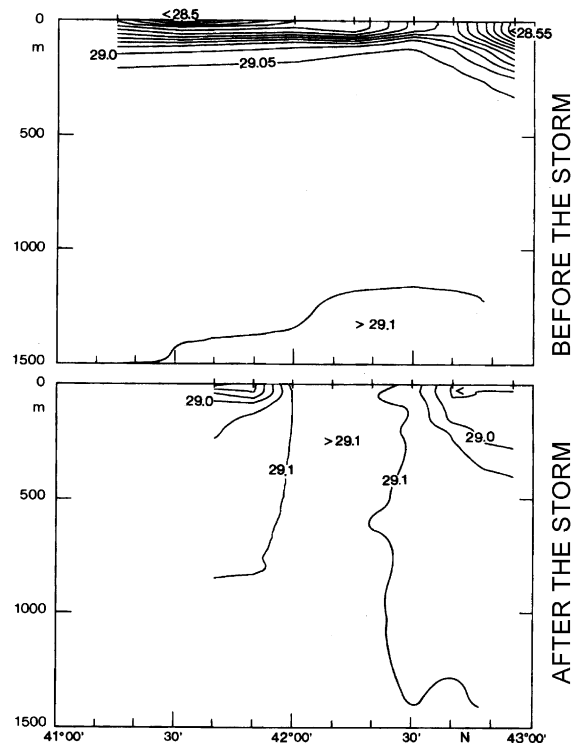

Fig. 2. Potential density (12–18 December 1991 and 20–22 February 1992) along 5°E of the Gulf of Lions before and after the storm (Schott et al., 1996).

measurements: only the experimental errors may be a source of uncertainty about its value. As regards the other quantities, the problem is more complex: the buoyancy flux $B_0 = \phi(\Delta\rho/\rho)g$ depends on the radiation, sensible and latent heat flux as well as on the sea water evaporation rate (the precipitation is disregarded here because this kind of event in the Mediterranean Sea is essentially due to dry winds). In addition, it generally varies in time and in space and is usually calculated by daily or weekly averages on thermal satellite or climatological data, so that its value varies according to the time range average process. The chimney's radius can also be estimated by meteorological or thermal satellite observations, subject to large uncertainty; the exact circular form is a theoret-

ical idealization and its estimated radius is the result of an averaging operation covering many directions. The stratification before the storm is never constant, neither vertically nor horizontally: the region has been preconditioned during the winter so that a large doming with uplifting isopycnals introduces a horizontal stratification that is larger at the boundary of the chimney than in its central part. The theoretical process leading to the VMJ, MN, Ch criteria do not take this aspect into account because a one-dimensional mixed layer Turner process is assumed for times $t < f^{-1}$. The stratification on the center of the chimney, where the horizontal stratification is weaker, is assumed in Eqs. (3) and (8a). It generally decays in depth, as clearly shown, for example, in Figs. 2 and 3,
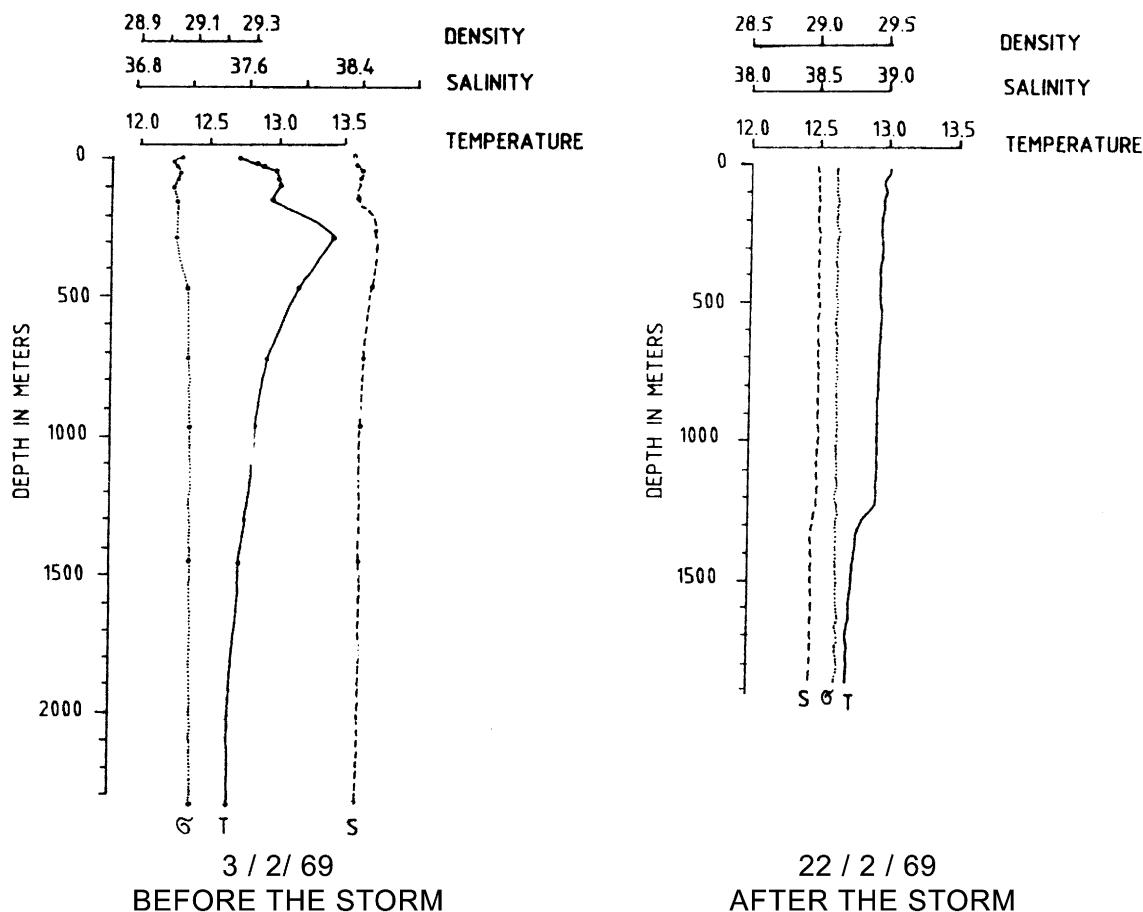

Fig. 3. Hydrological values versus depth (3 February 1969 and 22 February 1969) as measured by Dr. Frassetto's team in the Ligurian Sea before and after the storm.
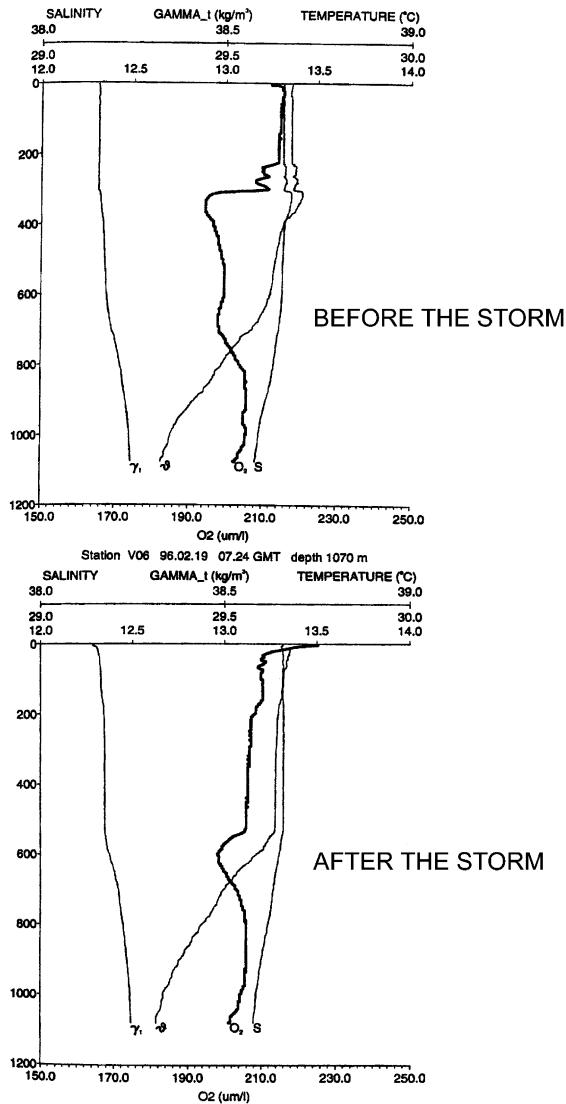
Fig. 4. Composition of vertical profiles of potential temperature (θ), salinity (S), density excess ($\gamma\theta$) and oxygen (O_2) at station V06 in the south Adriatic Sea before the storm (February 19) and after the storm (February 27) (from Manca and Bregant, 1998).

but a different stratification is shown, for example, in Fig. 4. The depth dependence of this quantity is ignored and the quantity,

$$N^2 = g \frac{\rho(h_f) - \rho(0)}{h_f \rho(0)} \qquad (9a)$$

has to be estimated from experimental measures. This procedure can be justified because the boundary

region, where the horizontal stratification is stronger, is the zone where the growing baroclinic instabilities are generated. The quantities N, R_0, B_0, h_f have been measured and calculated for some DWF events in the Mediterranean Sea: our data set, summarized in Table 1, has been taken from BNS and other references (Table 1.a). However, nothing may be said about the surface buoyancy flux decay region W: no field or satellite observation can lead to a satisfying estimate of this quantity. So a check of Eq. (3) can easily be made by means of a direct comparison between the measured and estimated depths shown in Table 2.a (like the BNS analysis). It has been already stressed in BNS that these are comparable within the errors (about 10–20% for h_{exp}, 30–40% for h_f) also if the VMJ criteria appear handier if the experimental quantities are measured in an uncontrolled condition like a real sea, because of the larger errors allowed. But this is impossible for the Ch Eq. (8a); consequently, one can only assume that W has the same order of magnitude as the error on R_0, but its value cannot be established exactly.

It is, however, possible to overcome this difficulty if the experimental data are used in order to calculate W from the Ch final mixing depth (Eq. (8a)), and then

Table 1
Data set analysed for the Mediterranean Sea

Region	Period	R_{exp} (10^4 m)	B_0 (10^{-7} m²/s³)	N (10^{-4} s⁻¹)	h_{exp} (10^3 m)
Gulf of Lions (1)	1987	7.0	4.3	5.5	2.0
(2)	1992	6.0	2.5	6.3	1.5
Ligurian (3a)	1969	3.0	5.0	7.0	1.2
(3b)	–	3.0	4.0	7.0	1.2
(4)	1991	4.0	5.0	10.0	0.8
Rhodes (5a)	1987	6.0	3.0	11.0	0.6
(5b)	–	6.0	3.0	11.0	0.7
(5c)	–	6.0	3.0	11.0	0.8
(5d)	–	6.0	3.0	11.0	0.9
(5e)	–	6.0	3.0	11.0	1.0
(6)	1990	8.0	2.0	11.0	1.0
(7)	1992	9.0	3.5	11.0	1.2
South Adriatic(8)	1956	2.0	2.6	9.0	0.6
North Aegean (9)	1987	4.0	3.5	13.0	0.6

The region and period columns show the site and the period of the DWF event; R_{exp}, B_0, N, h_{exp} are the experimental values of the radius, buoyancy flux, stratification and depth.

Table 1.a

References for data set shown in Table 1

Region	Period	References
Gulf of Lions (1)	1987	Schott and Leaman (1991)
(2)	1992	Schott et al. (1994); Thetis Group (1994); Send and Marshall (1995)
Ligurian (3a)	1969	Bunker (1972)
(3b)	–	–
(4)	1991	Spernocchia et al. (1995)
Rhodes (5a)	1987	Gertman et al. (1990)
(5b)	–	–
(5c)	–	–
(5d)	–	–
(5e)	–	–
(6)	1990	Gertman et al. (1994)
(7)	1992	Sur et al. (1992)
South Adriatic (8)	1996	Manca and Bregant (1998); Roether et al. (1996)
(9)	1987	Theocharis and Georgopoulos (1993)

to check its consistency with the Ch criteria (1) and (2) (namely to verify if $t^* \ll t_f$). So the quantity

$$\left(\frac{W}{R_{exp}}\right)^{1/4} = \frac{h_{exp} N \alpha^{1/4}}{(2fB_0 R_{exp}^2)^{1/4}} \quad (10)$$

can be estimated from Eq. (8a); then, in order to check if this value of W/R_{exp} corresponds to an internally or externally constrained event, it has to be put in Eq. (1):

$$
\begin{aligned}
t^* &= \frac{8}{9} \frac{f^2}{B_0} \frac{h_{exp}^8 N^8 \alpha^2}{(2fB_0 R_{exp})^2} \\
&= \frac{8}{9} \frac{f^2 R_{exp}^2}{B_0} \left[\left(\frac{W}{R_{exp}}\right)^{1/4}\right]^8
\end{aligned}
\quad (11)
$$

to be compared with:

$$t_f = \left(\frac{1}{2\alpha}\right)^{1/2} \left(\frac{fR_0 W}{B_0}\right)^{1/2} = \frac{h_{exp}^2 N^2}{2B_0} \quad (11a)$$

Here R_{exp} is the experimental value of the radius of the circular perturbed region and h_{exp}, B_0 are the experimental values for the final depth and the surface buoyancy flux inside it. The number W/R_{exp} (Eq. (10)) refers to the fraction of the circular region over which

the buoyancy flux is expected to decay in accordance with Eq. (8a) and the experimental data. In accordance with the Ch model, which fixes a transition time between two different regimes, the experimental values agree with the scale laws given in Eqs. (8a)–(8c) if $t^* \gg t_f$ or with the scale laws given in Eq. (3) or Eq. (6) if $t^* \ll t_f$. Note how the MN and VMJ scales assume a nonphysical discontinuity in B_0 on the boundary of the chimney such that by hypothesis $W = 0$. So the only way to check them is to compare directly the experimental and theoretical depths as shown in Tables 2.a and 2.b; if we define, for convenience, their ratio $h_{exp}/h_f = \lambda$, only if $t^* \ll t_f$ and $h_{exp}/h_f \sim 0(1)$ could these scaling laws be considered valid. The calculated values for n_t, h_{exp}/h_f, t_f, t^* using our data set (Table 1) are summarized in Table 2.b for each criterion separately. At first sight, it is $t^* \ll t_f$ for every event, so that no Mediterranean site among those analysed appears to be externally constrained: the time taken to reach the final quasi steady state is much longer than the transition time towards the internally constrained regime. This conclusion remains true with a very high probability also if t^* is estimated to have a very high error due to the high power of h_{exp} in Eq. (11): the really error on t^* is such that it seems impossible to infer anything by certainty about its real value, but its distance from t_f (whose

Table 2.a

The values of the final mixing depth h_M and h_V calculated by the Maxworthy and Visbeck criteria, respectively, compared with the experimental depths

Event	h_M (m)	h_V (m)	h_{exp} (m)
1	2000	2200	2000
2	1400	1500	1500
3a	1200	1400	1200
3b	1100	1300	1200
4	950	1000	800
5a	850	950	600
5b	850	950	700
5c	850	950	800
5d	850	950	900
5e	850	950	1000
6	800	900	1000
7	1000	1100	1200
8	700	750	600
9	650	700	600

The error on h_{exp} is about 10–20%; the error on the calculated quantities is greater. This table corresponds to the BNS table.

Table 2.b
The values of n_t (Eq. (2)) and λ from Table 2.a if $R_0 = R_{exp}$ for every event shown in Table 1

Event	N_t (10^{-1})	λ_M	λ_V	h_f^C (m)	t_f $(10^5$ s)	t_c^* $(10^5$ s)
1	1.6	1.0	0.9	2700	14.1	2.06
2	1.5	1.1	1.0	1900	17.9	4.24
3a	3.0	1.0	0.9	1700	7.05	0.88
3b	2.8	1.0	0.9	1600	8.82	1.62
4	2.5	0.8	0.8	1300	6.40	0.31
5a	1.6	0.7	0.6	1200	7.26	0.14
5b	1.6	0.8	0.7	1200	9.88	0.48
5c	1.6	1.0	0.9	1200	12.9	1.39
5d	1.6	1.1	1.0	1200	16.3	3.56
5e	1.6	1.2	1.1	1200	20.2	8.28
6	1.1	1.3	1.1	1100	30.2	15.7
7	1.3	1.2	1.1	1400	24.9	9.97
8	3.1	0.9	0.8	950	5.61	0.38
9	2.2	0.9	0.9	900	8.69	0.75

The subscripts M and V mean that they have been yielded with the Maxworthy and Visbeck values of β, respectively. h_f^C (Eq. (12)) is the minimum mixing depth possible with an externally constrained process; the last two columns show the corresponding process times (Eq. (11a)), and the transition times obtained from Eq. (11).

error is very small) is such that the estimated probability of an overlapping of the two time ranges is just about zero (by estimating 10–20% of error for h_f, 20% for B_0, 10% for N^2) for every event. In fact, by a rough estimate, it is:

$$t^* \simeq \left(1.0 \begin{array}{c} +5.0 \\ \\ -0.8 \end{array} \right) t_{av}^*,$$

so that the 'Medoc 1992' event (Table 2.b) shows an overlapping between the two time ranges, but appears to have an estimated lower than 30% probability to be externally constrained (if we assume a normal law of errors for h_{exp}, B_0, N^2 and t_f); except for the Rhodes event (1987e), it is impossible to infer such a probability. In some events (Rhodes 1990, 1992) for which the estimated left error on h_{exp} is about 25–50%,

$$t^* \simeq \left(1.00 \begin{array}{c} +5.00 \\ \\ -0.95 \end{array} \right) t_{av}^*$$

The overlapping between the two time ranges is such that it is very difficult to infer anything about the probability of constraint (external or internal). The values of W/R_{exp} consistent with these possible exter-

nally constrained events are $\gg n_t \sim O(10^{-1})$ (Table 2.b). They correspond to values of:

$$h_f^C \gg \left(\frac{2}{\alpha} \right)^{1/4} \frac{(fB_0 R_0^2 n_t)^{1/4}}{N} \quad (12)$$

shown in Table 2.b. It is evident at a glance that these expected depth values are very large, far from experimental values (but the errors on these values are also larger, about 50%), except at Rhodes site whose expected depth values remain comparable to them within the errors. Moreover, the values of λ appear to be $\simeq O(1)$ so that no further conclusion can be drawn about the MN and VMJ criteria than has been said by BNS.

Note that, by putting $R_0 = R_{exp}$, we have assimilated the quantities R_0, B_0 in the scaling laws with their mean experimental values. But B_0 is the result of a space–time average for which it is impossible to say whether it includes $B(r)$ on the boundary or not. Moreover, R_{exp} is estimated but has a large range of experimental error. A priori we cannot say if it includes or not the length interval of decreasing $B(r)$.

Indeed, the error sources are ~ 10–30% of the value of R_{exp}; not only is the measurement method a source of considerable error, but the chosen dimension is also obtained through a rough averaging operation over lengths in all directions. It is indeed very unlikely that the buoyancy flux region will really be circular. It is generally expected that the radius of the buoyancy flux region is deeply irregular, depending on the chosen direction so that a complex geometry could be considered as more realistic. If we set a circular geometry, we introduce a kind of abuse in our choice of the radius length: this is only rough and has a large error.

So the assumption $R_0 = R_{exp}$ introduces the systematic error of neglecting the experimental error in R_0 and the decreasing B_0 over its boundary, systematically underestimating its value. Ch has estimated the latter error as very small for $W/R_0 \leq 1$. In fact, the full integration of the surface buoyancy flux over the R large region gives the same equations (Eqs. (2) and (8a)–(8c)) with R_0 replaced by $R_0(1+(1/3)((W/R_0)^2/(1+(W/R_0)))) = O(R_0)$ (Chapman, 1998, Appendix). The condition $(W/R_0) > 1$ is not considered because in such a case, $Bu = (R_d/R_0)^2 > 1$ and baroclinic instability is not allowed.

Note that all of these considerations have been made roughly by knowing the calculated mean values and by estimating the errors of the measured quantities quoted in literature, so that arguments about covariance and correlation between the variables B_0 and R_{exp} cannot be made. So in general, it must be verified whether these conclusions are confirmed if the experimental R_{exp} are assumed to include the boundary region of decreasing $B(r)$, so that $R_{exp} = R$; that means we assume that the size of the region within which the maximum flux intensity B_0 has been calculated has been overestimated by an error of the same order of magnitude as the width size W. Appendix A and Table 3 show that, except for Rhodes, the transition time towards the internally constrained regime has a high probability to remain shorter than t_f for every examined event in the Mediterranean Sea even if we put $R_{exp} = R$. The region really swept by the winds is generally larger than the preconditioned region in which the buoyancy flux works in such a way that a greater and greater density is formed in a chimney. So the region where B_0 is decaying is mainly outside the chimney dimension. But, as noted before at the end of Section 2, the Mediterranean Sea is a well-stratified sea so that only a large W allows a Rossby radius $R_d < W$ (Eq. (9)) for deepwater events; only a less-stratified sea situated in a region of higher value of f could allow an externally constrained process. The east Mediterranean has a very high stratification, but the Rhodes gyre is very large and the winds blow up on a very larger extension, so that it could be possible that W is so large that an externally constrained process is allowed or that no criterion is satisfied for the convective process.

It may thus be argued that the W width and the Coriolis parameter are not scale variables for the chimney depth. But, while every site analysed, except Rhodes, appears internally constrained with a high probability, nothing else has been inferred about the VMJ and MN criteria.

4. About the process times

A problem generally pointed out in the literature is that the VMJ, MN models work only if the final process time is shorter than the meteorological perturbation time; the calculated t_f, summarized in Tables 2.b and 3, are generally longer, although not much longer than the meteorological time. For MN in a two-layer sea and BNS in a stratified sea, the Richardson number has to have a value lower than a critical one in order to allow the deepening process, so that a preconditioning process is necessary. The critical value of this number has been inferred from a laboratory experiment (MN) and is connected to the value of the efficiency parameter. The VMJ–MN laws depend on the buoyancy flux, the radius of the perturbed region, the stratification on the boundary, but do not depend on preconditioned quantities. The time of the process is calculated by assuming a uniform mixing layer deepening with a Turner law till the final quasi steady state: this is a real approximation that does not take into account any plume entrainment or reduced necessity for breaking a stratification in a preconditioned sea; neither the exchange of the fluid between the patch and the neighbouring water during the transient has been considered that lets the time grow to values higher than the physical ones also only if the minimum time is calculated. But it could be possible to say that the least time to the process is really shorter than Eq. (11a) but equal or longer than:

Table 3
The values of $n = W/R_0$

Event	n'_c (10^{-1})	n'_t (10^{-1})	t_f (10^5 s)	t^*_c (10^5 s)
1	0.5	1.8	14.1	2.28
2	0.6	1.6	17.9	4.82
3a	0.8	3.7	7.05	0.97
3b	1.1	3.4	8.82	1.99
4	0.3	2.9	6.40	0.34
5a	0.1	1.8	7.26	0.14
5b	0.2	1.8	9.88	0.50
5c	0.4	1.8	12.9	1.50
5d	0.6	1.8	16.3	4.05
5e	1.1	1.8	20.2	10.2
6	0.9	1.2	30.2	18.6
7	0.8	1.4	24.9	11.7
8	0.6	3.9	5.61	0.43
9	0.5	2.5	8.69	0.82

The values are from Appendix A for every event; t_f is the process time (Eq. (11a)), t^*_c are the transition times obtained in Appendix A.

$$t'_f = \frac{h_p^2 N_c^2}{2B_0} = \frac{h_p}{h_{exp}} t_f \left(1 + \frac{\Delta\rho^0_{cb}}{\Delta\rho_c}\right)^{-1} \qquad (13)$$

where h_p is the depth value of the final density anomaly isopycnal in the center of the preconditioned sea (before the last storm), N_c is the stratification in the center of the chimney, $\Delta\rho_c$ the density difference with the top and $\Delta\rho_{cb}^0$ is the surface horizontal density difference between the center and the boundary (in the preconditioned sea) within the final Rossby radius size; all these are their values before the last storm. The following argument can be used in order to get to Eq. (13): when the process is internally constrained, the quasi steady state is achieved if (following and modifying Jones and Marshall (1997) so as Chapman (1998) (Ch)):

$$\int \frac{\rho_0}{g} B_0 \mathrm{d}A = \int_{-h_f}^0 \oint \alpha v \Delta\rho \mathrm{d}l\mathrm{d}z \qquad (14)$$

But:

$$\Delta\rho = \frac{\rho_0 N_b^2}{g} h_f(1 + z/h_f) \qquad (15)$$

is the density difference across the front (depending on the stratification on the boundary), and

$$v \simeq N_c h_p \left(\frac{z^2}{2h_f^2} + \frac{z}{h_f} + \frac{1}{3} \right) \qquad (16)$$

is the velocity in the eddies; it depends on the stratification over the center and on h_p because it scales like the rim current at the onset of instability

Table 4
The values of the Rossby deformation radius (R_d), the Eady instability frequency (ω_{Eady}) and time (t_{Eady}) for every analysed event

Event	R_d (10^3 m)	ω_{Eady} (10^{-5} s^{-1})	t_{Eady} (10^4 s)
1	11.0	2.9	3.4
2	9.4	2.9	3.4
3a	8.4	3.5	2.8
3b	8.4	3.5	2.8
4	8.0	3.3	3.0
5a	6.6	2.0	4.9
5b	7.7	1.7	5.8
5c	8.8	1.5	6.6
5d	9.9	1.3	7.4
5e	11.0	1.2	8.2
6	11.0	1.2	8.2
7	13.2	1.0	9.9
8	5.4	3.6	2.7
9	7.8	4.3	2.3

Table 5
Calculated values of the stratification N in accordance with Eq. (9a), N_b on the boundary and N_c on the center of the "chimney" in accordance with their definition given in Section 4 for every analysed event

Event	N (10^{-4} s^{-1})	N_b (10^{-4} s^{-1})	N_c (10^{-4} s^{-1})
1	5.5	5.4	3.1
2	6.300	6.255	6.305
3a, 3b	7.0	7.6	10.3
4	10.0	10.5	9.9
5a–5e, 6, 7	11.0	11.1	8.9
8	9.0	9.9	6.6
9	–	–	–

when it is geostrophic and obeys to the thermal wind law. The instability time is very fast (Table 4), so that it is possible to say its beginning is about at the depth of h_p. So at the surface:

$$\frac{1}{2\alpha} \frac{\rho_0}{g} B_0 R_0 = h \frac{\rho_0}{g} N_b^2 h_f N_c \frac{h_p}{3} \qquad (17)$$

where $N_b^2 = (g/\rho_0)(\Delta\rho_b/h_{exp})$ is the boundary stratification (within the final Rossby deformation radius) and $N_c^2 = (g/\rho_0)(\Delta\rho_c/h_p)$ is the center stratification in the preconditioned sea. Differently from Ch, the value of the rim velocity has been taken proportional to $h_p N_c$, that is the buoyancy difference from the top to h_p. In fact, as told before, the horizontal density front is such that the boundary buoyancy flux due to baroclinic instability becomes predominant and can equal the surface buoyancy flux at about the preconditioned final density isopycnal depth; but:

$$\frac{N_b^2}{N_c^2} = \frac{h_p}{h_{exp}} \left(1 + \frac{\Delta\rho_{cb}^0}{\Delta\rho_c} \right) \qquad (18)$$

where $\Delta\rho_{cb}^0 = \rho_b(0) - \rho_c(0)$. By algebraic manipulations, it is easy to see that:

$$h_f = \left(\frac{3}{2\alpha} \frac{B_0 R_0}{N_b^3} \right)^{1/3} \frac{h_f}{h_p N_c/N_b}$$

$$= h_v \left[\frac{h_f}{h_p} \frac{1}{N_c/N_b} \right]^{1/3} \qquad (19)$$

where h_v is the final Visbeck depth. But

$$\frac{h_f}{h_p} \frac{1}{N_c/N_b} = \frac{h}{h_{exp}} \left(1 + \frac{\Delta\rho_{cb}^0}{\Delta\rho_c} \right) \frac{N_c}{N_b} \qquad (19a)$$

Table 6
The values of the restratification times for every event

Event	$t_{\mathrm{re}}^{\mathrm{J}}$ (10^5 s)	$t_{\mathrm{re}}^{\mathrm{pJ}}$ (10^5 s)
1	35.3	124
2	35.3	43.0
3a	19.8	29.3
3b	19.8	29.3
4	27.8	32.1
5a	50.5	75.8
5b	43.3	75.4
5c	37.9	75.4
5d	33.7	75.4
5e	30.3	75.8
6	40.4	100
7	37.9	113
8	20.6	37.4
9	28.5	71.1

The superscript J means that they have been calculated with the Jones values of the efficiency parameter; the superscript pJ means the same, but the velocity has been scaled with $N_c h_p$ instead of $N_b h_f$ (as shown in Section 4).

so that:

$$\left(\frac{h_{\exp}}{h_{\mathrm{f}}}\right)^{1/3} = \frac{h_{\exp}}{h_{\mathrm{v}}}\left(\frac{N_{\mathrm{b}}}{N_{\mathrm{c}}}\right)^{1/3} \quad (19\mathrm{b})$$

By using Eq. (18), it is immediate to yield Eq. (13). From now on, we put $N_{\mathrm{b}} = N$ because the two calculated values are about the same, as it is shown in Table 5.

It is to stress that the chimney water density anomaly reaches its final value when its depth in the center corresponds to the corresponding isopycnal depth in the preconditioned sea. As the chimney water depth reaches the value of the corresponding isopycnal in the preconditioned sea, the denser isopycnals are reduced to their natural depths and the dense water of the chimney adjusts at about the final h_{f} of the stratified sea through baroclinic instability (Legg et al., 1996) and patch breaking. A not very different argument was used by Legg et al. (1998) in their numerical work. So the value of the isopycnal depth h_{p} in the preconditioned sea is an important quantity to measure. The minimum time (Eq. (13)) is connected to the inferred final mixing depth by:

$$h_{\mathrm{f}}^2 h_{\mathrm{p}} = \frac{B_0 R_0}{N^2}\frac{1}{2\alpha}\frac{1}{N_{\mathrm{c}}} \quad (20)$$

If a constant $\epsilon < 1$ is defined so that $h_{\mathrm{p}} = \epsilon h_{\exp}$, the inferred final mixing depths appear generally deeper, because the ratio between the experimental final depth and its theoretical value defined in Eq. (20) $\lambda' = h_{\exp}/h_{\mathrm{f}}'$ is:

$$\lambda' = \epsilon^{1/4}\lambda^{3/2}\left(1 + \frac{\Delta\rho_{\mathrm{cb}}^0}{\Delta\rho_{\mathrm{c}}}\right)^{1/4} \quad (21)$$

where $\lambda = h_{\exp}/h_{\mathrm{f}}$ has been defined in Section 3.

Table 7
Data set for the preconditioned sea for every analysed event ($\epsilon = h_{\mathrm{p}}/h_{\exp}$) in the center

Event	ϵ	$\Delta\rho_{\mathrm{b}}/\rho_0$ (10^{-3})	$\Delta\rho_{\mathrm{c}}/\rho_0$ (10^{-3})	$\Delta\rho_{\mathrm{bc}}/\rho_0$ (10^{-3})	h_{fM}' (m)	h_{fV}' (m)	t_{f}' (10^5 s)	$t_{\mathrm{c}}'^*$ (10^5 s)
1	0.5	0.06	0.01	0.05	1700	2000	1.172	0.057
2	0.8	0.06	0.05	0.01	1300	1500	11.91	2.949
3a	0.46	0.07	0.06	0.01	1300	1500	2.782	0.608
3b	0.46	0.07	0.06	0.01	1200	1400	3.478	1.187
4	0.84	0.09	0.07	0.02	1000	1200	4.181	0.191
5a	0.8	0.05	0.04	0.01	1000	1100	4.646	0.089
5b	0.7	0.05	0.04	0.01	900	1000	5.534	0.306
5c	0.6	0.05	0.04	0.01	900	1000	6.195	0.889
5d	0.55	0.05	0.04	0.01	850	1000	7.187	2.282
5e	0.5	0.05	0.04	0.01	800	950	8.067*	5.301
6	0.5	0.05	0.04	0.01	750	900	12.10*	10.06
7	0.4	0.05	0.04	0.01	1000	1200	7.965*	6.379
8	0.8	0.06	0.02	0.04	600	750	1.495	0.043
9	–	–	–	–	–	–	–	–

$\Delta\rho_{\mathrm{b}}$, $\Delta\rho_{\mathrm{c}}$ are the vertical density difference between the top and the density anomaly isopycnal at the boundary and at the center of the chimney; $\Delta\rho_{\mathrm{bc}}$ is the surface horizontal density difference and the corresponding values of t_{f}' (Eq. (13)), t'^* (Eq. (A.3.5)), h_{fM}', h_{fV}' (Eq. (21)). The asterisk signs (*) mean the times shorter than the transition times t_{c}^* in Table 2.b; the subscripts M and V mean the quantities calculated with the MN, VMJ values of β, respectively.
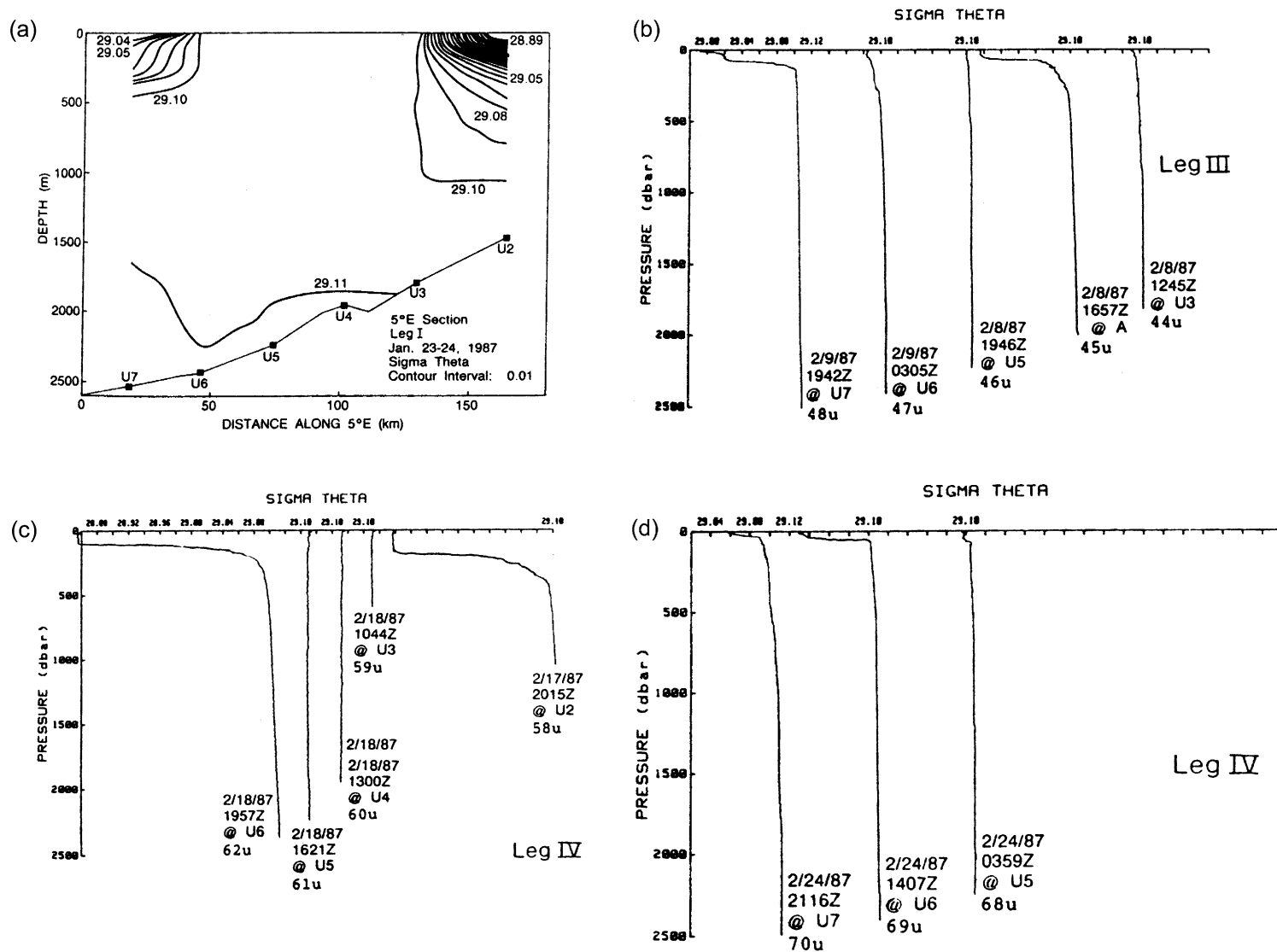
Fig. 5. (a) Cross sections of potential density along 5°E on 23/24 January 1987 (before the last event); note that a well-defined homogeneous patch is already present before the last event. (b) CTD profiles of potential density along 5°E on 8/9 February 1987. (c) Same as (b), but for 17/18 February. (d) Same as (b), but for 24 February (from Leaman and Schott, 1991).

It should be noted that h_{exp} has generally been measured after the end of the storm (it is difficult to do measurements during the storm), but before the final restratification process. The restratification time t_{re} is generally estimated very long, as analysed by Jones and Marshall (1997); they show that:

$$t_{re} = \frac{\beta R_0}{2Nh_f} \qquad (22)$$

depending on the efficiency parameter and on the velocity scale Nh_f. The values of t_{re} for every analysed event are shown in Table 6 (in the same table, the same quantities calculated with a scale of velocity equal to $N_c h_p$ are also shown). So it is understandable that the experimental deepwater depth is sometimes slightly deeper, sometimes slightly shallower than its inferred final depth. In fact, the isopycnals are horizontal only in a restratified sea: nothing says that the bottom of the chimney region in the final quasi steady state is flat, but steep isopycnals are still allowed.

The calculated t_f' are summarized in Table 7; these times are shorter, so that they become comparable to the meteorological times. In any case, these last times appear longer than the Eady instability times $t_{Eady} = (N^2 h_{exp} \rho_0)/(0.3g\Delta\rho_b f) \simeq 3f^{-1}$ (Appendix B), when a meandering process starts to appear along the boundary (Table 4). A comparison between Table 7 and transition times summarized in Tables 2.b and 3 shows that the comparison relation between the mean final and transition times generally does not change. By taking into account the preconditioning, the transition times are less lowered (see Eq. (A.3.5)) than the process times. The consequence is that, by taking into account the errors, the overlapping between the two time ranges increases and the probability of externally constrained events grows a bit; but the assumed deepwater events in the Rhodes gyre (1987e, 1990, 1992) can be so fast that the minimum time becomes so near the transition time, that in such a case, it is impossible to draw a conclusion about the kind of constraint (internal or external). Moreover, here, the Eady instability time appears longer than $3f^{-1}$ (Table 4). The case of the Medoc 1987 event is different; it is very fast because it is the last of some recurring, very strong, events following one another that have deeply homogenized the water during the winter (Fig. 5). A large deformation radius was thus present already at the beginning of the last concluding process. In any case, it is possible to conclude that, if it is:

$$\frac{h_p}{h_{exp}} \sim \frac{N^2}{N_c^2(pr.)} \frac{1}{1 + \frac{\Delta\rho_{cb}^0}{\Delta\rho_c}} = \epsilon$$

the inferred final mixing depth will be between Eqs. (3) and (21). It should be noted that Straneo and Kavase (1999) has yielded a different relation for t_f:

$$t_f = \frac{h^2(N^2 - \frac{M^2}{f}(\frac{M^2}{f} - f^*))}{2B_0}$$

depending on M^2 (the horizontal boundary stratification in the preconditioned sea) and on the vertical and horizontal Coriolis parameters.

5. Conclusion

We have analysed the experimental data referring to events leading to deepwater formation in some known Mediterranean sites in order to check the Ch model concerning the criteria to use to infer their depth. We may conclude that it is very possible to say that all of the analysed DWF sites, except the Rhodes site, are internally constrained. About the VMJ and MN criteria, the BNS conclusions are generally confirmed, but a check of the times of the process allows to identify some corrections to criteria (Eq. (19)) and give some insight on the processes time scales too. Every physical quantity has been measured (as it is possible to argue from a rough analysis of Rhodes data) in an uncontrolled situation so that errors of even 50% may be expected for the final mixing depth. However, every error in the data amplifies the error in the quantity sought. Also, the error in the dimension of the cooling region is underestimated in our equations.

In particular, as stressed in BNS, the values of the buoyancy flux are computed by the ECMWF tables where daily or monthly averages have been made. The error in B_0 is important (see, for example, the Ligurian case where a small change from 4×10^{-7} to 5×10^{-7} m^2/s^3 gives different results). It is perhaps possible to reduce the effect of the error in B_0 if a new criterion can be obtained by taking the space and time stochas-

tic variability of B_0 into due consideration. A first attempt in this direction was made in Bouché (2000a, b,c).

Of the analysed Mediterranean deepwater sites, the Rhodes region appears questionable. Generally, the theoretical depths appear much shallower than the experimental ones and our analysis shows no consistency with the theoretical expectations, showing even a too long instability time. Moreover, it is not possible to draw any conclusion about the kind of constraint (internal or external).

In the present work, a rough attempt to suggest some new broader criteria that would also indicate the process times has been made. They identify new important quantities to be known and measured accurately in a field observation, that is, the ratio ϵ (connected to preconditioned quantities) defined before in the last paragraph. The introduction of the quantity ϵ does not change the estimated depths calculated within an error much larger than the error on the experimental depths, but considerably lets the estimated process times down, so that they may be comparable to the meteorological times; so the process may be checked by a crossed depth and time analysis. In such a way, the times for the deepwater events at the Rhodes gyre become so short that could conceivably be considered as externally constrained events (50%). The questionable results about the Rhodes events may be due to an incorrect evaluation of the experimental data (as the analysis of the 1987 event suggests), or to a different physical process (for example, entrainment from the bottom). Anyway, it should be noted that the preconditioned stratification has been estimated from averaged winter values mapped in the Atlas, because there are no measures for the two analysed events. But it is also likely that the other two cooling events, incompatible with every criterion, are not to be considered deepwater formation events, but only intermediate or levantine water formation, or that the process times ($t^* \approx t_f$) are such that no criterion is good. It is necessary to have new field data regarding other events in order to draw some conclusions.

In order to reduce the effect of the error on the size of the cooling region so as to take into account the stochastic variability of B_0, it may be admissible to seek a more complex geometry (for example, a stochastic dependence of R_0 on the direction) instead of a circular one, although this certainly cannot be the main problem for the comprehension of the Rhodes events. The situation is more hopeful if the variability of B_0 and the depth dependence or horizontal variability of N^2 are taken into account. A study that takes into account the depth dependence of N^2 and its horizontal variability was undertaken in a numerical work (Straneo and Kavase, 1999). A study that considers the evolution of water patches from the beginning, when a stochastic variability of B_0 is taken into account, has been undertaken in Bouché (2000a,b,c). Anyway, a deeper analysis of the phenomenon has to be made. In my future work, I shall investigate the possibility of obtaining new criteria according to the above suggestions. In any case, it must be stressed that it is impossible to give exact laws for inferring field measures in such an uncontrolled situation in a sea before and after a storm.

Acknowledgements

Appendix A

If we raise Eq. (8a) to the fourth power, we obtain:

$$h_{exp}^4 = \frac{2}{\alpha} \frac{fB_0 R_o W}{N^4}$$

so that, if $R_0 = R_{exp} - W = R - W$, from Eq. (7), it is: $R_0 = (R/(1+n)) = (R_{exp}/(1+n))$ where $n = (W/R_0) = ((W/R_{exp})(1+n))$, so that $W = nR_0 = ((nR_{exp})/(1+n))$.

By simple algebraic manipulations, we have:

$$n = \frac{h_{exp}^4 \alpha N^4}{2fB_0 R_{exp}^2}(1+n)^2 = \gamma(1+n)^2 \qquad \text{(A.1.1)}$$

whose solution is:

$$n_c = \frac{1}{2\gamma}(1 - 2\gamma \pm \sqrt{1 - 4\gamma})$$

In order to check the kind of constrainment (internal or external) of each event, one has to use criterion (2) and to compare n_c to:

$$n_t = \left(\frac{9}{8}\right)^{2/3} \left(\frac{1}{2\alpha}\right)^{1/3} \frac{B_0^{1/3}}{fR_{\exp}^{2/3}} (1 + n_t)^{2/3} \qquad (A.1.2)$$

The calculated values for n_t, n_c, t_f together with the transition times t_c^* (for $n = n_c < 1$) for the BNS data set (Table 1), are summarized in Table 3. The solution $n_c > 1$ is not to be taken into account because it gives too large decay region no longer consistent with Eqs. (8a)–(8c). In fact, a large value for n_c would mean considering a condition in which the experimental errors on $R_{\exp}$ are greater than the mean value.

Appendix B

It is known that:

$$\omega_{\text{Eady}} = \frac{0.3f}{\sqrt{Ri}} = \frac{0.3f}{N} \frac{dv}{dz}$$

where Ri is the Richardson number. But the thermal wind law allows to say that:

$$\omega_{\text{Eady}} = = \frac{0.3}{N} \frac{g}{\rho_0} \frac{\partial \rho}{\partial r} = \frac{0.3g\Delta\rho_{\text{bc}}}{NR_d}$$

But at the equilibrium, the chimney density is given by the bottom density, so that it is possible to say that:

$$\omega_{\text{Eady}} = \frac{0.3 \, g\Delta\rho_b f}{N^2\rho_0 h_f}$$

Appendix C

During the steady state, it is:

$$\frac{\rho_0}{2\alpha g} B_0 R_0 = hv\Delta\rho \qquad (A.3.1)$$

In an externally constrained event, if the sea is preconditioned, it is possible to say that v scales like the velocity along the rim current at the onset of instability when the rim current velocity v_g is nearly

geostrophic and can be estimated from the thermal wind balance:

$$\frac{\partial v_g}{\partial z} \sim \frac{2v}{h_p} = -\frac{g}{\rho_0 f} \frac{\partial \rho}{\partial r} \qquad (A.3.2)$$

where $\partial\rho/\partial r = (\rho_0 N_c^2/g)(\partial h_p/\partial r)$. By algebraic manipulations, remembering that $\Delta\rho = (\rho_0 N_b^2 h)/g$, it is:

$$h^4 = h_c^4 \left(1 + \frac{\Delta\rho_{\text{cb}}}{\Delta\rho_c}\right) \qquad (A.3.3)$$

so that:

$$\left(\frac{W}{R_0}\right)^{1/4} = \frac{h_{\exp}N\alpha^{1/4}}{(2fB_0R_{\exp}^2)^{1/4}} \left(1 + \frac{\Delta\rho_{\text{cb}}}{\Delta\rho_c}\right)^{-1/4} \qquad (A.3.4)$$

If we put this equation in Eq. (1), we obtain:

$$t'^* = \frac{t^*}{\left(1 + \frac{\Delta\rho_{\text{cb}}}{\Delta\rho_c}\right)^2} \qquad (A.3.5)$$

References

Anati, D.A., 1984. A dome of cold water in the Levantine Basin. Deep-Sea Research 31, 1251–1257.

Bouché, V., 2000a. Statistical convective down motion driven by random inputs of localized buoyancy in a homogeneous sea. Nuovo Cimento 23C (5), 469–485.

Bouché, V., 2000b. On a statistical approach of convective motions in the sea driven by random buoyancy inputs on a homogeneous and non homogeneous viscous sea. Journal of Marine Research (submitted for publication).

Bouché, V., 2000c. Stochastic approach to convective motions driven by a localized buoyancy flux in the sea. Proceed.-Actes-NhaTrang 2000 Int. Coll. Mech. Sol. Fluids Inter. (Aug. 14–18). LTAS, Université de Liège, Belgium, pp. 156–168.

Bunker, A., 1972. Wintertime interaction of the atmosphere with the Mediterranean Sea. Journal of Physical Oceanography 2, 226–238.

Buongiorno-Nardelli, B., Salusti, E., 1999. On dense water formation criteria and their application to the Mediterranean Sea. Deep-Sea Research. Part 1. Oceanographic Research Papers 47 (2000), 193–221.

Chapman, D.C., 1998. Setting the scales of the ocean response to isolated convection. Journal of Physical Oceanography 28, 606–620.

Coates, M.J., Ivey, G.N., Taylor, J.R., 1995. Unsteady, turbulent convection into a rotating, linearly stratified fluid: modeling deep ocean convection. Journal of Physical Oceanography 25, 3032–3050.

Georgopoulos, D., Theocharis, A., Zodias, G., 1989. Intermediate

water formation in the Cretan Sea (south Aegean Sea). Oceanologica Acta 12, 353–359.

Gertman, I.F., Ovchinnikov, I.M., Popov, Y.I., 1990. Deep convection in the Levantine Sea. Rapp. P.v. Reun. Commun. Int. Mer. Medit. 32, 172.

Gertman, I.F., Ovchinnikov, I.M., Popov, Yu.I., 1994. Deep convection in the eastern basin of the Mediterranean Sea. Oceanology 34 (1), 19–25.

Gremes Cordero, S., 1999. The use of thermal satellite data in dense water formation studies in the Mediterranean Sea. Journal of Marine Systems 20, 175–186.

Jones, H., Marshall, J., 1993. Convection with rotation in a neutral ocean: a study of open-ocean deep convection. Journal of Physical Oceanography 23 (6), 1009–1039.

Jones, H., Marshall, J., 1997. Restratification after deep convection. Journal of Physical Oceanography 27, 2276–2287.

Killworth, P.D., 1983. Deep convection in the world ocean. Reviews of Geophysics and Space Physics 21 (1), 1–26.

Lascaratos, A., 1993. Estimation of deep and intermediate water mass formation rates in Mediterranean Sea. Deep-Sea Research 40, 1327–1332.

Leaman, K.D., Schott, F.A., 1991. Hydrographic structure of the convection regime in the Gulf of Lions: winter 1987. Journal of Physical Oceanography 21, 575–598.

Legg, S., Jones, H., Visbeck, M., 1996. A Heton perspective of baroclinic Eddy transfer in localized open ocean convection. Journal of Physical Oceanography 26, 2251–2266.

Legg, S., Mc Williams, J., Gao, J., 1998. Localization of deep ocean convection by a Mesoscale Eddy. Journal of Physical Oceanography 28, 944–970.

Manca, B., Bregant, D., 1998. Dense water formation and circulation in the southern Adriatic Sea during winter 1996. Rapport-Commission Internationale de la Mer Mediterranee 35, 176–177.

Marshall, J., Schott, F., 1998. Open-ocean convection; observations, theory and models. Review of Geophysics 17 (1), 1–64.

Marshall, J., Whitehead, J.A., Yates, T., 1994. Laboratory and numerical experiments in oceanic convection. In: Malanotte-Rizzoli, P., Robinson, A.R. (Eds.), On Ocean Processes in Climate Dynamics: Global and Mediterranean Examples. Kluwer Academic Publishing, Dordrecht, pp. 173–201.

Maxworthy, T., 1997. Convection into domains with open boundaries. Annual Review of Fluid Mechanics 29, 327–371.

Maxworthy, T., Narimousa, S., 1994. Unsteady, turbulent convection into a homogeneous, rotating fluid, with oceanographic applications. Journal of Physical Oceanography 24, 865–887.

MEDOC Group, 1970. Observation of formation of deep water in the Mediterranean Sea. Nature 227, 1037–1040.

Narimousa, S., 1996. Penetrative, turbulent convection into a rotating, two layer fluid. Journal of Fluid Mechanics 312, 295–313.

Narimousa, S., Maxworthy, T., 1994. The interaction of unsteady, rotating convection with a density interface. Ocean Modelling 103, 4–5.

Ovchinnikov, I.M., Zats, V.I., Krivosheya, V.G., Udodov, A.I., 1985. Formation of deep eastern Mediterranean waters in the Adriatic Sea. Oceanology 25, 704–707.

Ozturgut, E., 1976. The source and spreading of the Levantine Intermediate Water in the eastern Mediterranean. Saclant ASW Research Center Memorandum SM-92, La Spezia, Italy, 45 pp.

Roether, W., Manca, B., Klein, B., Bregant, D., Georgopoulos, D., Beitzel, V., Kovacevic, V., Luchetta, A., 1996. Recent changes in Eastern Mediterranean deep waters. Science 271, 333–335.

Schott, F., Leaman, K., 1991. Observations with moored acoustic Doppler current profilers in the convection regime in the Golfe du Lion. Journal of Physical Oceanography 21, 558–574.

Schott, F., Visbeck, M., Fisher, J., 1993. Observations of vertical currents and convection in the central Greenland Sea during the winter of 1988–1989. Journal of Geophysical Research 98 (C8), 14401–14421.

Schott, F., Visbeck, M., Send, U., 1994. Open ocean deep convection, Mediterranean and Greenland seas. In: Malanotte-Rizzoli, P., Robinson, A.R. (Eds.), On Ocean Processes in Climate Dynamics: Global and Mediterranean Examples. Kluwer Academic Publishing, Dordrecht, pp. 203–225.

Schott, F., Visbeck, M., Send, U., Fischer, J., Stramma, L., Desaubies, Y., 1996. Observations of deep convection in the Gulf of Lions, northern Mediterranean, during the winter of 1991/92. Journal of Physical Oceanography 26 (4), 505–524.

Send, U., Marshall, J., 1995. Integral effects of deep convection. Journal of Physical Oceanography 25 (5), 855–872.

Spernocchia, S., Picco, P., Manzella, G., Ribotti, A., Copello, S., Brasey, P., 1995. Intermediate water formation in the Ligurian Sea. Oceanologica Acta 18 (2), 151–162.

Straneo, F., Kavase, M., 1999. Comparison of localized convection due to localized forcing and to preconditioning. Journal of Physical Oceanography 29, 55–68.

Sur, H.I., Ozsoy, E., Unluata, U., 1992. Simultaneous deep and intermediate depth convection in the northern Levantine Sea, Winter 1992. Oceanologica Acta 16 (1), 33–43.

Theocharis, A., Georgopoulos, D., 1993. Dense water formation over the Samothraki and Limnos Plateau in the North Aegean Sea (Eastern Mediterranean Sea). Continental Shelf Research 13 (9), 919–939.

Thetis Group, 1994. Open-ocean deep convection explored in the Mediterranean Sea. EOS, Transactions of the American Geophysical Union 75 (19), 217–221.

Tzipermann, E., 1996. On the role of interior mixing and air–sea fluxes in determining the stratification and circulation of the oceans. Journal of Physical Oceanography 16, 680–693.

Visbeck, M., Marshall, J., Jones, H., 1996. Dynamics of isolated convective regions in the ocean. Journal of Physical Oceanography 26, 1721–1734.

Dr. Vanda Bouché is a researcher on Theoretical Physics at the Department of Physics of the University of Rome "La Sapienza". During her research life, she has been interested in statistical physics, fluids dynamics, the greenhouse effect and oceanography.